CFD BASED SIMULATION OF HYDROGEN RELEASE THROUGH ELLIPTICAL ORIFICES

Shishehgaran, N., Paraschivoiu, M.
Department of Mechanical and Industrial Engineering, Concordia University,
1515 St. Catherine St. West, Montreal, Quebec, H3G1M8, Canada,
n_shish@encs.concordia.ca, paraschi@encs.concordia.ca

ABSTRACT

Computational Fluid Dynamics (CFD) is applied to investigate the near exit jet behavior of high pressure hydrogen release into quiescent ambient air through different types of orifices. The size and geometry of the release hole can affect the possibility of auto-ignition. Therefore, the effect of release geometry on the behavior and development of hydrogen jet issuing from non-axisymmetric (elliptical) and expanding orifices is investigated and compared with their equivalent circular orifices. A three-dimensional in-house code is developed using the MPI library for parallel computing to simulate the flow based on an inviscid approximation. Convection dominates viscous effects in strongly under-expanded supersonic jets in the vicinity of release exit, justifying the use of the Euler equations. The transport (advection) equation is applied to calculate the concentration of hydrogen-air mixture. The Abel-Nobel equation of state is used because high pressure hydrogen flow deviates from the ideal gas assumption.

This work effort is conducted to fulfill two objectives. First, two types of circular and elliptic orifices with the same cross sectional area are simulated and the flow behavior of each case is studied and compared during the initial stage of release. Second, the comparative study between expanding circular exit and its fixed counterpart is carried out. This evaluation is conducted for different sizes of nozzle with different aspect ratios.

1.0 INTRODUCTION

Hydrogen and electricity are the two competing future energy sources for the transportation industry. The main advantage of hydrogen over electricity is the short refuelling time, nevertheless, as high pressure reservoirs are used, concerns about safety need to be addressed. Accidental release of hydrogen from high pressure reservoirs can lead to auto-ignition or to dispersion of a hydrogen cloud. It was shown that for each storage pressure there exists a size of the hole that separates the non-ignition region from the self-ignition region [1]. Very detailed direct numerical simulation DNS results, done for small release pressures and for long release tubes, lead to similar conclusions [2] [3]. Other studies have focused on the dispersion of hydrogen to calculate the concentration of hydrogen for the release hole and to analyse how the concentration is affected by the diameter of the circular hole [4]. In many of these studies Computational Fluid Dynamics (CFD) was used and it was shown to be a powerful tool that provides good agreement with experimental data [5]. In this study, the near exit jet is studied using CFD as this is the critical location for auto-ignition. The novelty of this work is that the influence of exit geometry (circular, elliptical and expanding) on the flow and later on auto-ignition is investigated.

Indeed, most of the studies about hydrogen safety issues were focused on the circular nozzles and on the development of hydrogen jet exiting from a standard round exit. Penaeu et al [6] investigated the hydrogen release from the circular nozzle with the pressure of 10 MPa using an ideal gas law. The deviation of hydrogen behaviour from the ideal gas rises with increasing pressure as shown by Mohamed et al [7]. He used the Beattie–Bridgeman state equation to describe specific heats, internal energy and speed of sound. Khaksarfard et al [8] applied the Abel Nobel equation of state to study the incident release of pressurized hydrogen from the storage at P= 70 MPa into ambient air. So, in the current study a real gas model is applied due to the high pressure storage of 70 MPa.

Among the earliest researches on asymmetric jets is the work by Krothapalli et al [9]. They investigated incompressible jets through rectangular and elliptical nozzles with aspect ratios greater than 5.5. The results show that non-circular jet increases the mixing capability. Makarov and Molkov [10] simulated the under-expanded hydrogen jet for circular and plane nozzle using the Ideal gas equation. The hydrogen was released from the reservoir at 35 Mpa and the aspect ratio of the plane nozzle was set to 200. It was shown that the plane nozzle jet causes faster mixing in comparison to the round nozzle in the vicinity of the release area. The axis-switching phenomenon was observed during the simulation. The phenomenon produces a rotation of the jet axes, so the major axis becomes the minor axis further downstream. It was appeared that the hydrogen concentration for both cases with the same mass flow rate drops to the low flammability of 4% at the same location in downstream. The main objective of the present work is to numerically study the effect of orifice geometry on the hydrogen jet behaviour during the incident release from pressurized tank at 70 MPa into ambient air. Three cases are evaluated, elliptical, circular and expanding orifices. First, the results of elliptical orifices are compared with the circular opening, and then, the expanding exit is examined compared to fixed round exit. The total areas of the comparable orifices in the first evaluation is assuming constant. Elliptic orifices, especially the orifices with higher aspect ratio can be considered as a model of crack, and also the expanding exits can simulate the real scenario of crack growth. So study the structure of highly under-expanded jet issuing from these types of orifices leads to the precise evaluation of incident release of hydrogen into the ambient air.

2.0 GOVERNING EQUATIONS

2.1 Euler Equations

In this study, due to the high Reynolds number in the vicinity of the release hole, the effect of viscosity is ignored and flow is modeled by the compressible Euler equations. Considering the dynamic mesh formulation in which the convecting velocity is the relative velocity with respect to the stationary frame, the modified conservative form of the Euler equations in the absence of any source terms, will be as follows:

$$\frac{\partial \vec{U}}{\partial t} + \vec{\nabla}.\vec{\vec{F}}(U) = 0, \tag{1}$$

$$\vec{U} = \begin{bmatrix} \rho \\ \rho u \\ \rho v \\ \rho w \\ \rho E \end{bmatrix}, \vec{\vec{F}} = \left(\begin{bmatrix} \rho(u - w_x) \\ \rho(u - w_x)u + P \\ \rho(u - w_x)v \\ \rho(u - w_x)w \\ \rho(u - w_x)E + uP \end{bmatrix} \begin{bmatrix} \rho(v - w_y) \\ \rho(v - w_y)u \\ \rho(v - w_y)v + P \\ \rho(v - w_y)w \\ \rho(v - w_y)E + vP \end{bmatrix} \begin{bmatrix} \rho(w - w_z) \\ \rho(w - w_z)u \\ \rho(w - w_z)v \\ \rho(w - w_z)w + P \\ \rho(w - w_z)E + wP \end{bmatrix} \right) \tag{2}$$

Where $\vec{U}$ is the vector of conservative variables and $\vec{\vec{F}}$ represents the convective fluxes. The vector of primitive variables is $\vec{W} = \begin{bmatrix} \rho \\ u \\ v \\ w \\ P \end{bmatrix}$. w_x, w_y, w_z are the grid speeds along the coordinate directions, which represent the time rates of change of the position vectors. In the case of fixed mesh, the grid velocities are not considered and the cell volume is not time-dependant and does not change by time. To simulate the hydrogen jet escaping through the expanding orifices, the dynamic mesh model based on the spring analogy is used. This method is described in [8].

2.2 Transport (Advection) Equation

To describe the convection of the hydrogen into the ambient air, the advection equation is implemented.

$$\frac{\partial c}{\partial t}+\frac{\partial (cu)}{\partial x}+\frac{\partial (cv)}{\partial y}+\frac{\partial (cw)}{\partial z}=0 \quad (3)$$

This equation, while being solved, is segregated or decoupled from the Euler equations. It means that at the end of the each time step and after solving the linear system of equations by iterative GMRES solver [11], the advection equation is solved separately by the same solver. After calculating c, the average value of the gas constant, *R*, for the hydrogen-air mixture is solved by equation (4).

$$R = R_{H_2}(1-c)+R_{air}c \quad (4)$$

Where $R_{H_2} = 4124\ J/kgK$ and $R_{air} = 287\ J/kgK$.

The specific heats are assumed to be constant throughout the release, thus, γ=1.4. The air mixture fraction is defined as 1 and hydrogen mixture fraction is 0.

2.3 Real gas Equation of State

Owing to the high pressure flow (P_i=70MPa), Abel Nobel real gas equation is utilized to calculate the temperature profile. The accuracy of this equation is almost the same as the more complicated real gas equations such as Beattie-Bridgeman but its simplicity reduces the solution time and computational cost [12].

$$p = (1-b\rho)^{-1}\rho RT, \qquad b = 0.00775\ m^3/kg \quad (5)$$

3.0 NUMERICAL TECHNIQUE

In this study, only the initial level of hydrogen release and near exit jet is investigated. The flow is simulated and solved by three-dimensional finite volume Euler equations using an in-house parallel code. This code has been extensively validated and demonstrated good agreement with experimental results for a wide variety of CFD problems [13]. The system of non-linear equations is solved by means of a fully implicit scheme which has an accuracy of the first and second orders in time and space, respectively. Convective fluxes are evaluated using Roe-MUSCL scheme. This method is among the most efficient schemes to calculate the convective fluxes at the boundaries especially for Euler simulations, but the oscillations can be generated near the shock or discontinuity regions. To avoid this problem, the Van Leer-Van Albada limiter is applied. The limiter controls the accuracy of spatial approximation at the thin layer near the exit hole (|Z|=0.1orifice diameter) and high pressure gradient regions where the second order approximation is switched to the first order accuracy to prohibit the numerical instabilities in this regions.

To simulate the expanding release hole, the dynamic mesh based on the spring analogy method is used to update the volume mesh. Therefore, the relative velocities in each coordinate direction are added in all governing equations. Then the system of equations is solved using an iterative GMRES solver and MPI parallel processing to reduce the solution time.

4.0 COMPUTATIONAL MODEL

The 3D computational domain shown in Figure 1(a) consists of a circular cylinder as a reservoir containing hydrogen gas at high pressure and a 2mm straight nozzle leading to the exit at the ambient pressure. To examine the influence of orifice geometry on the behaviour of gas and ignition possibility, three different shapes of orifices are considered, circular, elliptic and expanding exits.

4.1 Elliptical and Circular Orifices

The parameter under consideration for comparable circular and elliptical orifices is the same exit area. Therefore, three different areas based on 1 mm, 2 mm and 5 mm diameters of circular exits are assumed. For each case, two varying elliptical shapes with the aspect ratios (major axis/minor axis) of

AR=4 and AR=6 are figured out and compared with their comparable circular counterparts (AR=1).

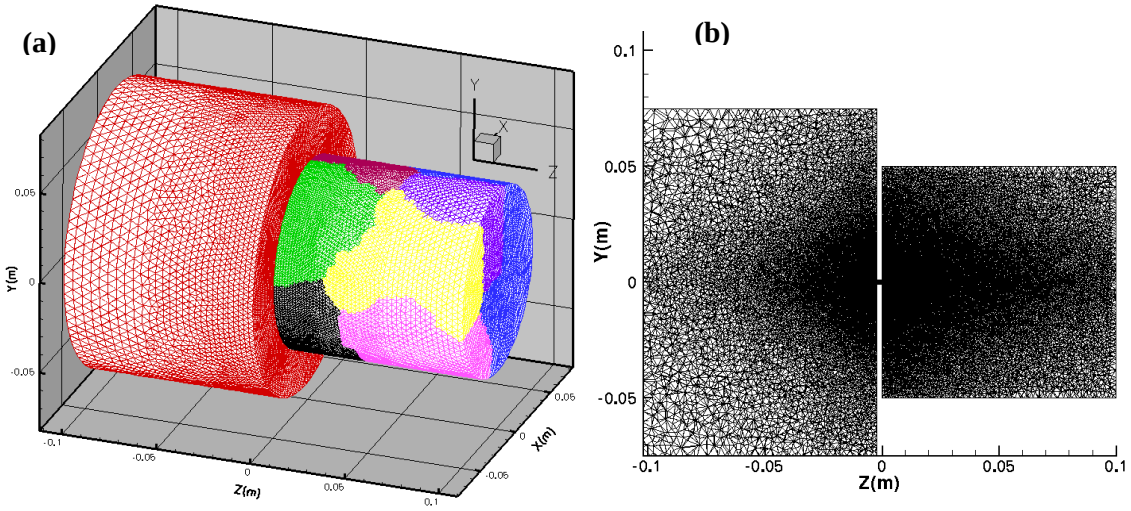

Figure 1: The computational domain with unstructured tetrahedral mesh, a) the discretized domain with decomposed zones using METIS (partially shown), b) 2D slice of the computational domain

The dimensions of the all test cases are listed in Table 1 and the cross sectional surfaces of exit geometries of AR=1, AR=4 and AR=6 with the identical area of A=19.63 mm^2 is depicted in Figure 2. The minor axis in all elliptical cases is perpendicular to the axial axis of the pressurized tank.

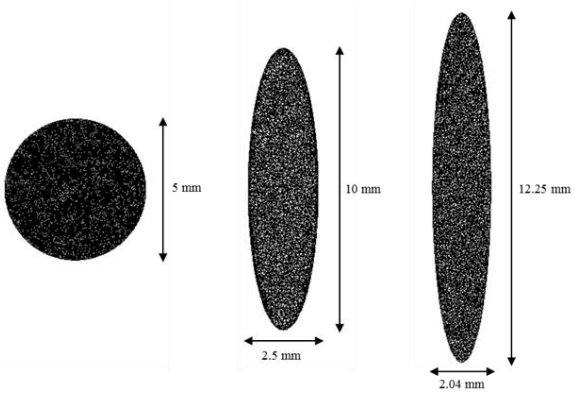

Figure 2: The cross sectional surfaces of the varying ARs of the orifices with the equal exit area

4.2 Expanding Orifices

Two cases of round orifice with initial diameters of D_i=1 mm and D_i=2 mm are considered to evaluate the expanding exit and compare the results to the fixed circular opening with the same initial diameters. The length of the release tube is equal in all cases.

The discretized domain contains almost 2 million nodes and 12 million tetrahedrons. To ensure that the mesh is sufficiently refined to resolve large pressure gradients and all relevant flow features, a very fine grid resolution is generated in the proximity to the exit area. Then, to reduce the solution time and computational cost, the element size increases with a growth rate of 1.02 in downstream and in the regions far from the exit (Figure 1(b)). METIS software package is used to distribute the finite element mesh to the processors and partition the domain for parallel computing. The computational domains are decomposed up to 64 partitions. Parallel computation is run on Cirrus (Concordia University Cluster) and Mammouth-parallel II supercomputers.

As mentioned before, the viscosity effect and the heat transfer between the gas inside the reservoir and its surrounding are neglected, therefore all the solid walls of the high pressure tank are assumed to be

slip-free and adiabatic. A constant pressure boundary condition was applied around the circumference of the low pressure cylinder (external environment) and at the end of the cylinder.

Table 1: Dimensions of different types of orifices

Area(A)=0.8 (mm^2)			
Orifice Type	Major Axis, a(mm)	Minor Axis, b(mm)	Aspect Ratio, a/b
Circular	1	1	1
Elliptical 1	2	0.5	4
Elliptical 2	2.45	0.41	6
Area(A)=3.14 (mm^2)			
Orifice Type	Major Axis, a(mm)	Minor Axis, b(mm)	Aspect Ratio, a/b
Circular	2	2	1
Elliptical 1	4	1	4
Elliptical 2	5	0.82	6
Area(A)=19.63 (mm^2)			
Orifice Type	Major Axis, a(mm)	Minor Axis, b(mm)	Aspect Ratio, a/b
Circular	5	5	1
Elliptical 1	10	2.5	4
Elliptical 2	12.25	2.04	6

5.0 RESULTS

The discussion is broken down by comparing, first, the hydrogen release through a fixed elliptical orifice in comparison with its circular counterpart, and second, the gas release through a circular expanding hole compared to the fixed round hole. The flow is initially at rest with zero velocity. The reservoir and the half of the tube filled with hydrogen at the pressure of 70 MPa and the rest with air at the atmospheric pressure. The initial temperature of the domain is 300 K. As the effects of orifice geometry and aspect ratio on the gas jet and auto-ignition are significant only in the near field flow and diminish in the far field, this study focuses on the near exit jet behaviour.

5.1 Fixed Elliptic Orifice in Comparison with Circular Orifice

To study the influence of release hole geometry on the hydrogen jet behaviour near the exit area, two elliptic orifices with AR=4 and AR=6 are compared with the circular orifice with AR=1 (Table 1). To investigate this effect on different dimensions of release hole, three different effective areas are considered. The length of the release tube is 2 mm and it is preserved in all cases.

One of the important parameter to determine the ignition possibility is the pressure expansion at the interface of hydrogen and air. Therefore, the centreline pressure versus time on the contact surface for circular and elliptical exits with different diameters is compared together up to a time of 10 μs (Figure 3(a, b and c). It is observed that by maintaining the same effective area and increasing the aspect ratio of release hole, pressure on the contact surface expands more rapidly during the initial release time. This behaviour can be negligible for the area of 0.8 mm^2, while it is crucial for the larger orifice size (Area=19.63 mm^2). It means that elliptical exit with the small area behaves like its comparable circular hole. In addition, it is recognized that the smaller release holes have a more pronounced expansion and a steeper pressure gradient which cause the hydrogen jet reaches ambient pressure in a short time.

To evaluate the release time, when the hydrogen-air interface reaches the exit hole (z=0), the contact surface location versus time along the centreline for the orifice size of Area=3.14 mm^2 is plotted in Figure 3(d). It is evident that the release time corresponding to varying geometries is virtually equal and it is t=0.6 μs. It is noticed in Figure 3(b), when the gas escaping into the air, after a short delay, the interface pressure starts expanding with time.

Distribution of Mach number and concentration after 10 micro seconds for circular and elliptical (AR=4) orifices with the equivalent area of A=3.14 mm^2 are presented in Figures 4.

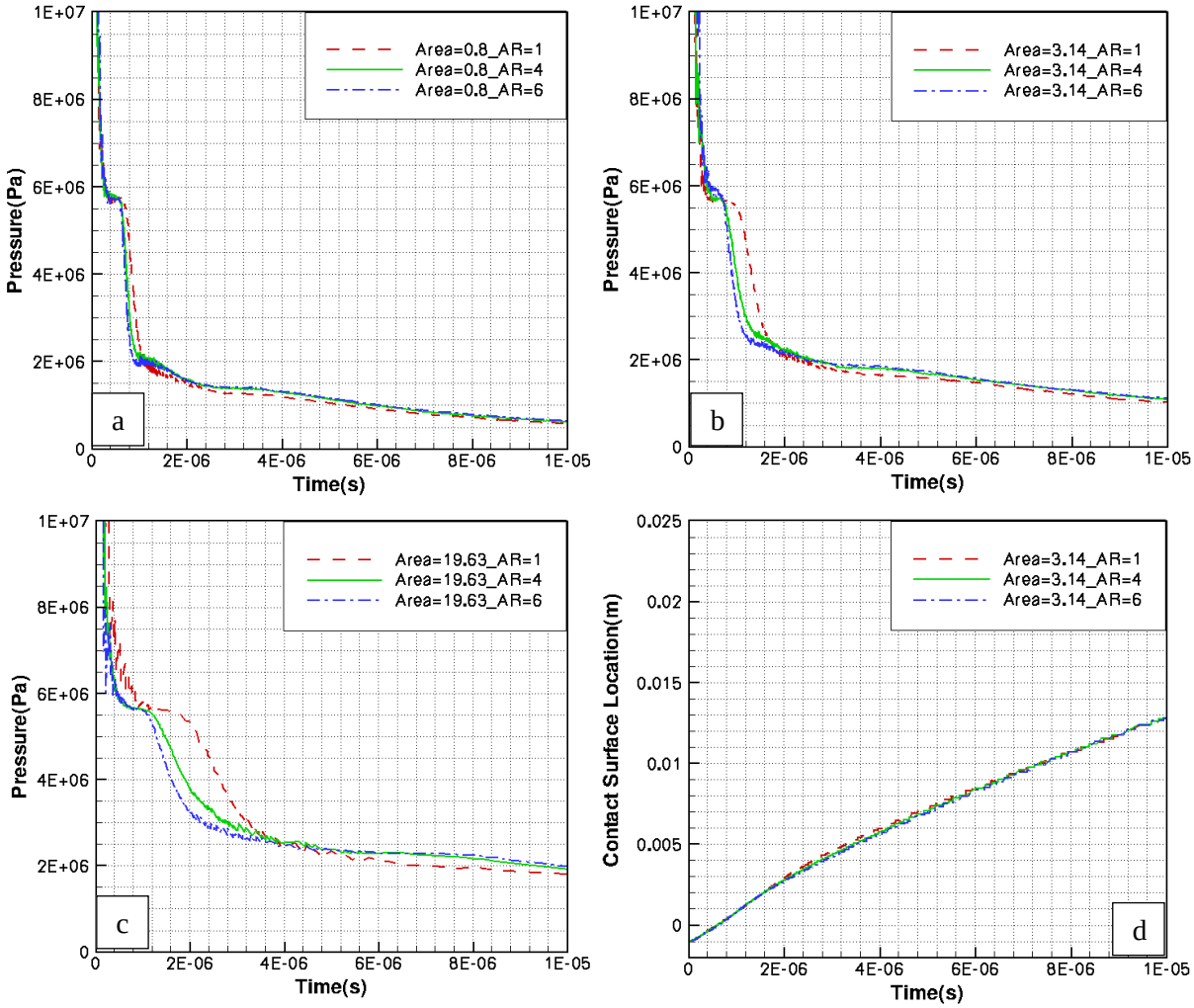

Figure 3: Contact surface pressure versus time for different aspect ratios of release hole, AR=1, AR=4 and AR=6 a) Area=0.8mm^2, b) Area=3.14mm^2, c) Area=19.63mm^2, d) the comparison of contact surface location versus time of elliptical and circular orifices (Area=3.14 mm^2)

By comparing the Mach number and concentration along the minor and major axes, it is understood that the change in the orifice geometry affects the development of the jet. Spreading and mixing characteristics differ from elliptical and circular jets. Hydrogen jet releasing from the elliptical hole spreads more quickly in the minor axis plane than the major axis plane and, in turn, it mixes with air faster along the minor axis and advances through the ambient air more quickly. While the circular hydrogen jet spreads with the same rate in both directions and the mixing rate does not change along the minor and major axes. The unequal spreading rates are because of the non-uniform curvature variation.

Figure 5 shows the centreline temperature at different times for both circular (AR=1) and elliptical (AR=4) orifices with the Area=3.14 mm^2. In both cases, temperature has the maximum peak before hydrogen releases into the air and the hydrogen-air interface reaches the exit (t<0.6 μs). As it is shown, the maximum peak is determined at t=0.2 μs. After the leakage of hydrogen into the air, the maximum temperature starts decaying with time. The values of temperature inside the release tube and even at the release time, for both cases are virtually the same, but during the expansion time, circular orifice has a higher temperature than the elliptical as seen at 1 μs. It is because of the difference in expansion

rate. As it was shown in Figure 3(b), contact surface pressure corresponding to elliptic cases decreases faster in comparison with its comparable circular case, and at t=1μs has a lower value. However, inside the low pressure environment, due to the better mixing of elliptic jet compared to circular, the temperature related to elliptical exit is slightly higher.

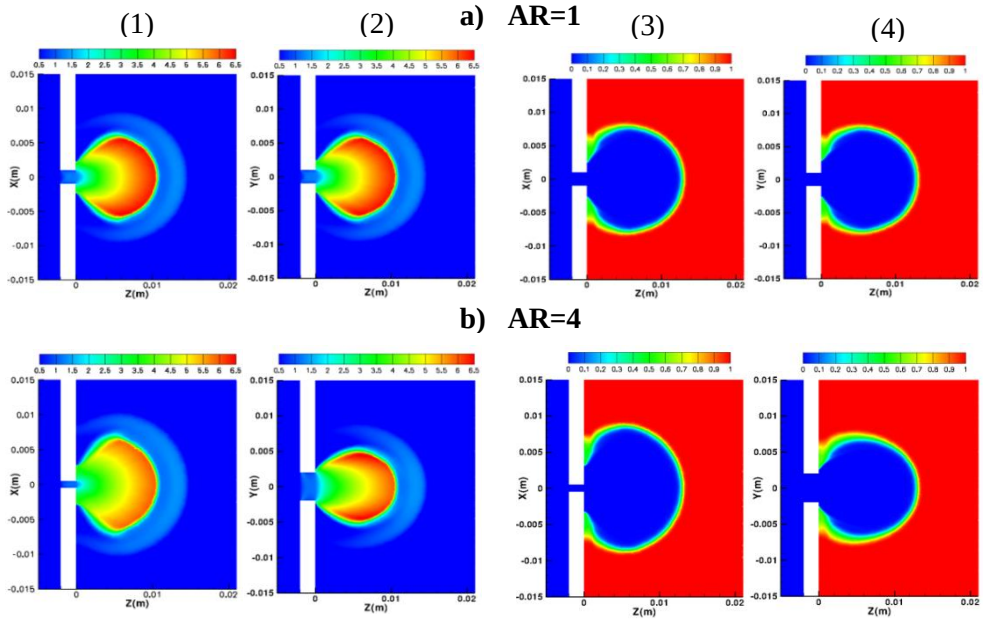

Figure 4: Mach number and concentration after 10 μs of hydrogen release into air from the circular and elliptical orifices (Area=3.14 mm^2), a) AR=1, b) AR=4, 1) Minor axis plane, Mach Number, 2) Major axis plane, Mach Number, 3) Minor axis plane, Concentration, 4) Major axis plane, Concentration

Centerline Mach number, concentration, temperature and pressure of different aspect ratios of the orifice with the area of A=3.14 mm^2, after 10 μs are compared in Figure 6. The locations of the Mach disk and air-hydrogen contact surface do not change with varying aspect ratios. The contact surfaces are located practically at the same distance of about z=13 mm for all cases. While the maximum Mach number changes for varying aspect ratios and it is noticed that the lower the aspect ratios, the stronger the Mach disk. As the area of the opening increases, the difference between the contact surface locations regarding different aspect ratios grows but it is insignificant for the orifices with the smaller area. The temperature and pressure profile do not change significantly, however the maximum temperature is slightly higher for the orifice with the higher aspect ratio.

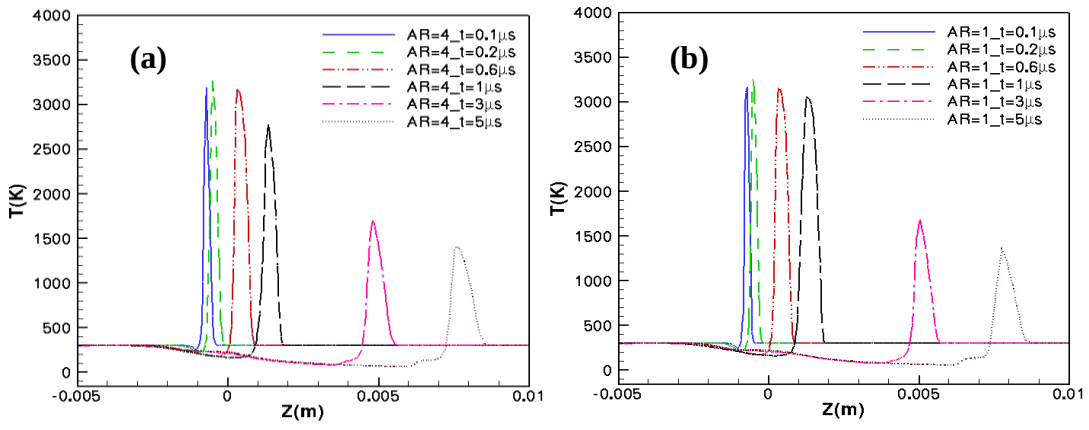

Figure 5: Temperature along the centreline at different times before and after the hydrogen release (Area=3.14 mm^2), a) Elliptical orifice b) Circular orifice

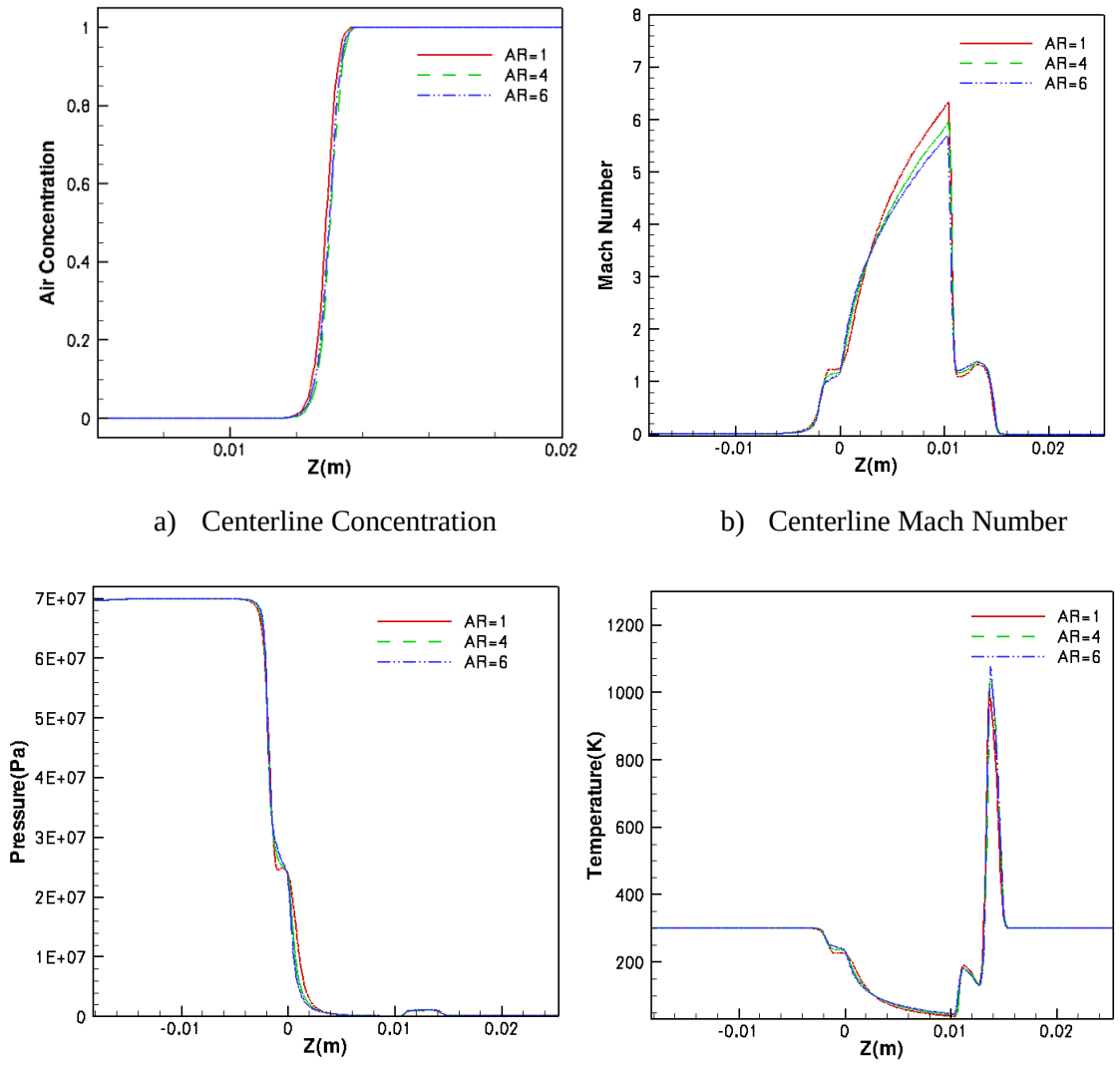

a) Centerline Concentration

b) Centerline Mach Number

c) Centerline Pressure

d) Centerline Temperature

Figure 6: a) Concentration, b) Mach Number, c) Pressure and d) Temperature along the centreline after t=10μs of hydrogen release into air from the circular and elliptical orifices (Area=3.14mm^2)

4.2 Expanding circular release hole in comparison with fixed circular opening

To evaluate the influence of orifice deformation on the hydrogen jet, enlarging circular orifice is simulated. The results of expanding circular orifices are compared with the fixed cases with the identical initial diameters. Two initial diameters of 1 mm and 2 mm with the expanding rate of 0.2 mm/μs are studied. The two dimensional mesh slices of the expanding release hole with initial diameter of 2 mm at several times after discharging the hydrogen into air are illustrated in Figure 7.

The location of contact surface during the initial 4 μs and the pressure versus time for initial diameter of D=1 mm and D=2 mm are compared respectively in Figure 8(a) and Figure 8(b). In all cases, the hydrogen-air interface reaches the exit at t=0.6 μs. As it is seen, the contact surface pressures related to expanding release geometries decays sharply after the leakage into the ambient air in comparison with their fixed counterparts. This behaviour is started from t=0, i.e., before the interface of the hydrogen-air comes out of the exit hole, the rate of pressure decay is affected by the enlarging release tube, and, as a result, the pressure starts to drop more rapidly in comparison with the constant release area. In addition, the pressure on the interface of hydrogen and air releasing through the smaller area drops more sharply than the larger area. This pattern is similar to the fixed cases (elliptical, circular) which

were illustrated in Figure 3.

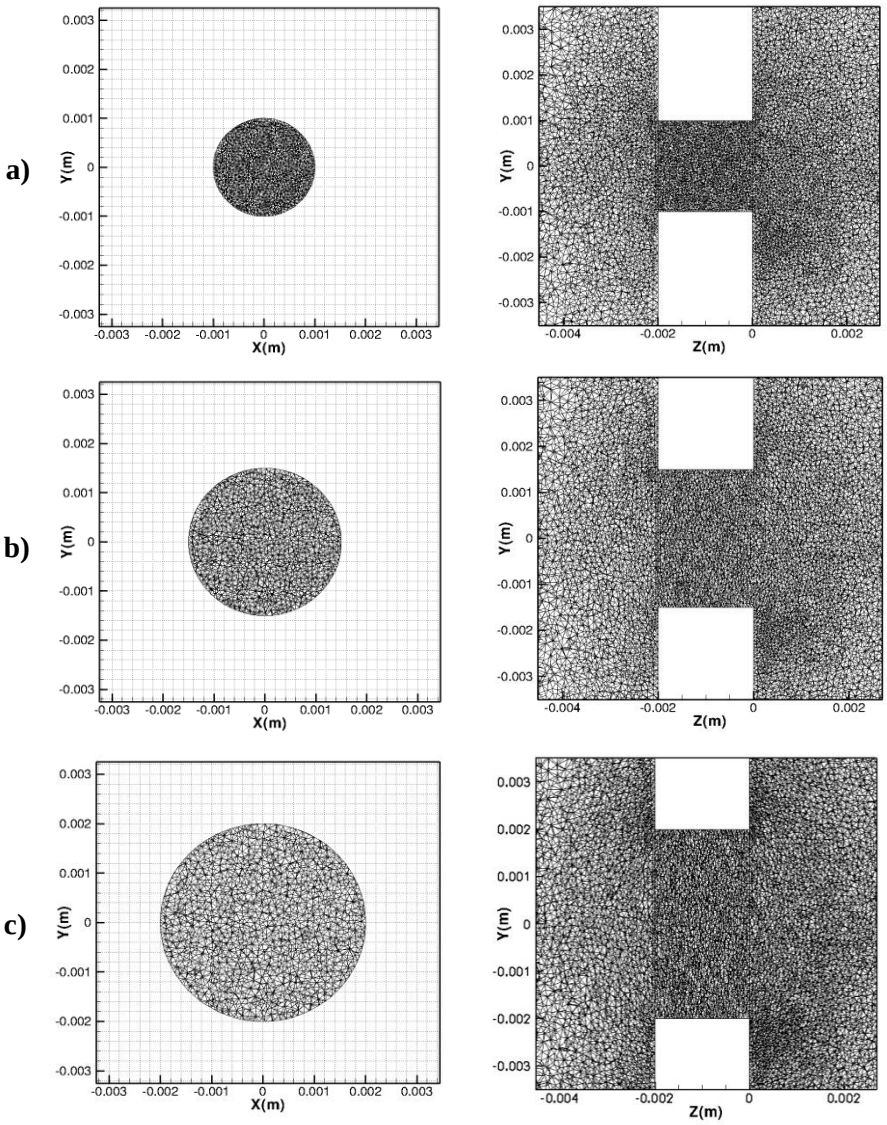

Figure 7: Two dimensional views of the expanding release hole (D_i=2mm, v=0.2mm/μs), x-y plane (left), y-z plane (right), a) t=0 (initial diameter), b) t=5 μs, c) t=10 μs

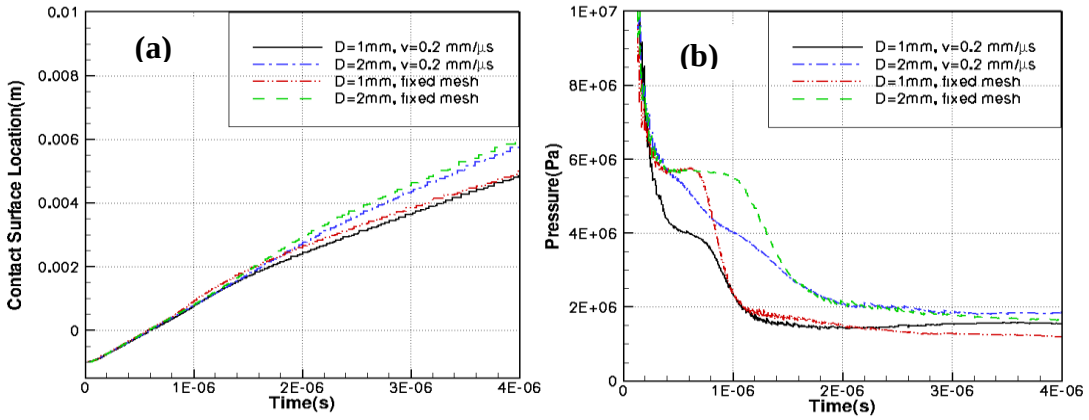

Figure 8: The comparison of a) contact surface location versus time b) Hydrogen-air contact surface pressure versus time of expanding and fixed orifices (D_i=1 mm and D_i=2 mm)

After the discharging of hydrogen into air and starting the pressure expansion, the contact surface location of fixed hole develops rapidly relative to their equivalent expanding case, since the velocity of the gas is higher when it escapes from the fixed opening (Figure 8(a)). It is noticed that the difference between the lead contact surface location of enlarging orifice and constant orifice is getting higher by time.

Figure 9 presents the centreline distribution of concentration, Mach number, pressure and temperature of expanding and fixed circular orifices with the initial diameter of 2 mm, after the t=5 μs. It is seen that the locations of the Mach disk and contact surface in both cases are slightly affected. The Mach disk is situated at $Z=4.25D_i$ and the hydrogen-air interface location stands on $Z=3.5D_i$. It is because the high expansion velocity prevails over the release hole expanding rate, in turn, the varying orifice does not affect the location of Mach disk and hydrogen-air contact surface. The strength of the Mach disk related to the orifice with constant area is stronger than the Mach disk of enlarging orifice. The lower and upper peaks of the temperature are slightly affected by the expanding release hole at t=5 μs. It can be recognized that the centreline pressure drops more quickly through the expanding orifice from the tank pressure (70 MPa) to the environmental pressure compared to the fixed opening.

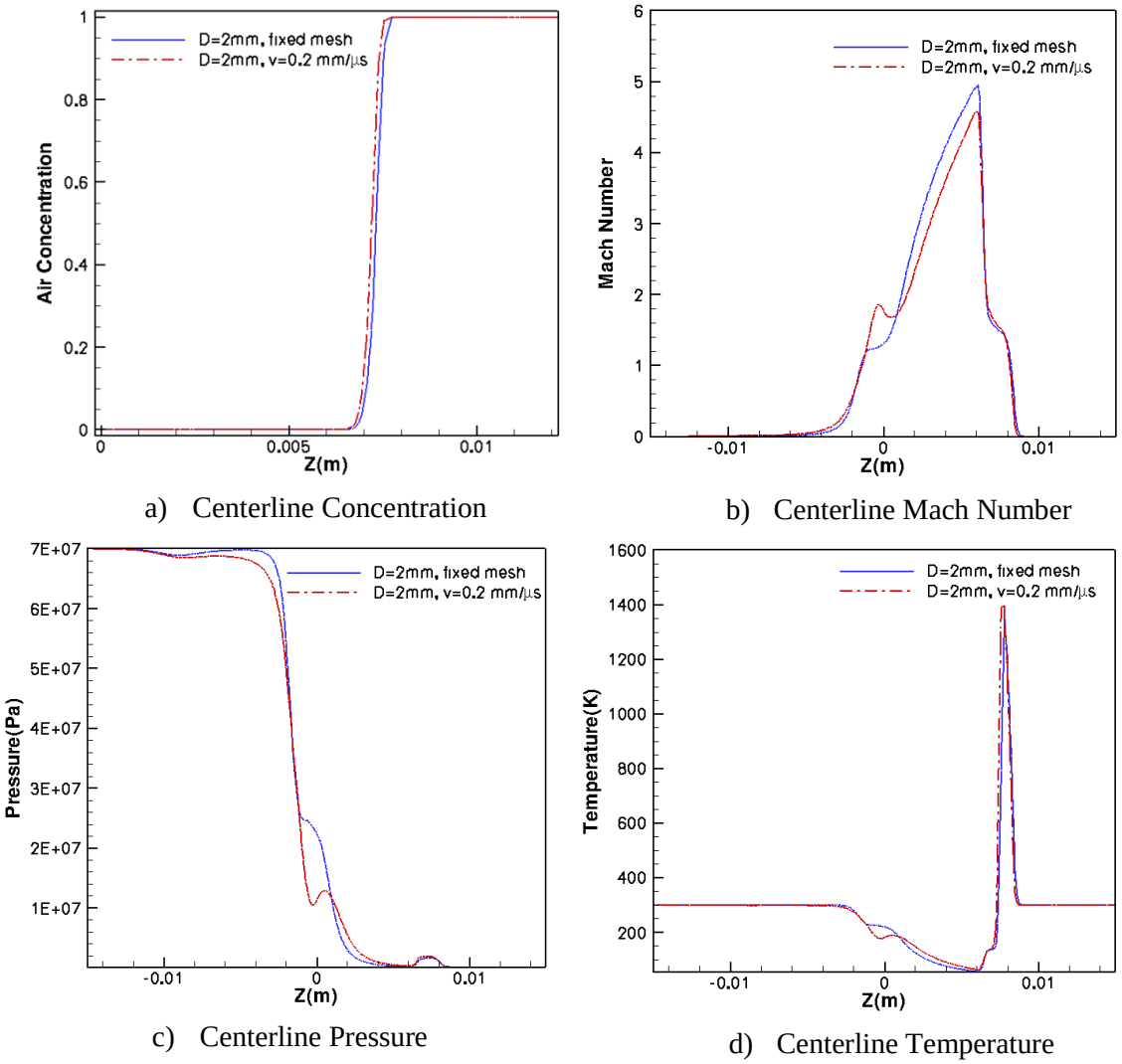

a) Centerline Concentration

b) Centerline Mach Number

c) Centerline Pressure

d) Centerline Temperature

Figure 9: a) Concentration, b) Mach Number, c) Pressure and d) Temperature along the centreline after t=10μs of hydrogen release into air from the expanding and fixed orifices (D_i=2mm)

Figure 10 shows the centreline temperature of expanding orifice at several times. Similar to the fixed

cases, the maximum peak of the temperature is located in the release tube; however in this case, it is occurred sooner. The expansion rate of contact surface pressure in expanding case is higher than the fixed case, in turn; the temperature started decreasing sooner and faster. It is noticed, at the release time, both cases have practically the same value of temperature peak, but after discharging the hydrogen jet and during the expansion (at t=1 μs), since the contact surface pressure in the enlarging orifice case decays more sharply; it has a lower peak of temperature compared to fixed orifice. Therefore, it can be concluded, due to the higher pressure expansion and lower temperature peak in expanding case, the possibility of auto-ignition is less than the fixed case.

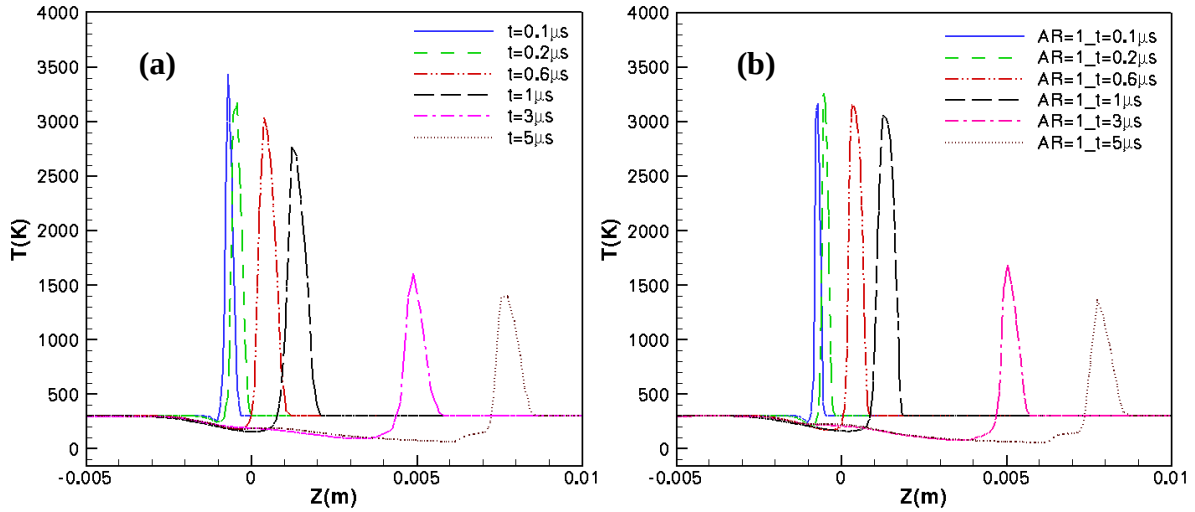

Figure 10: Centreline temperature at several times before and after the hydrogen release (Area=3.14 mm^2), a) expanding exit b) fixed circular exit

4.0 CONCLUSIONS

The high-pressure release of hydrogen into quiescent air from different types of orifices was investigated using an in-house parallel code. As convection dominates viscous effects in strongly under-expanded supersonic jets near the release exit, flow was modelled by the compressible Euler equations. Since the critical location of auto-ignition is in the near field flow, in this study, only the near exit jet was simulated. This work has been conducted to serve two purposes; first, two types of circular and elliptical orifices with the equivalent effective area were considered and the effects of these geometries of orifices on the flow behaviour were compared. Second, the comparative study between expanding circular exit and its fixed counterpart was carried out. In the first approach, different sizes of orifices (Area=0.8 mm^2, Area=3.14 mm^2, Area=19.63 mm^2) with varying aspect ratios of AR=1, AR=4 and AR=6 were examined.

The transport (advection) equation was used to calculate the concentration of hydrogen-air mixture. The Abel-Nobel equation of state was applied to calculate the flow temperature. The pressure of the reservoir and initial temperature of the domain were set to 70 MPa and 300 K respectively. The static air was at the atmospheric pressure.

It was recognized that the contact surface pressure was affected by the geometry and dimensions of the orifice. By comparing the fixed elliptical and circular orifices, it is concluded, as the aspect ratio of the orifice increases, the contact surface pressure decreases and expands more rapidly. Therefore, the contact surface pressure of the elliptical jet decays more quickly than the comparable circular jet. The same comparison between expanding and round orifices has shown that the enlarging exit starts decaying sooner than the fixed circular opening. Thus, the contact surface pressure depends on both dimensions and the geometry of the release hole. The temperature profile and peak values before and after the hydrogen releases into the air were investigated. It was observed that in all cases, the maximum peak of temperature was occurred in the release tube. All cases had virtually the same peak

value at the release time with slightly difference. During the expansion, the temperature related to the fixed circular orifice was higher than its comparable value in elliptic exit case. It is because, the contact surface pressure drops more sharply in elliptic case compared to the fixed circular case. The same behavior was recognized in the case with expanding orifice. Due to the high pressure expansion rate of expanding orifice in comparison with fixed round exit, the upper peak of temperature in this case decreases more quickly and has a lower value during the expansion time. Therefore, it can be concluded, the expanding case has a less probability of auto-ignition compared to its fixed orifice counterpart. The contact surface location and Mach disk location are slightly changed by applying different geometries of release hole.

ACKNOWLEDGEMENTS

This work is supported by the NSERC hydrogen Canada (H_2CAN) Strategic Research Network.

REFERENCES

1. Maxwell, B.M. and Radulescu, M.I., Iignition limits of rapidly expanding diffusion layers: Application to unsteady hydrogen jets, *Combustion and Flame Journal*, **158**, No. 10, 2011, pp. 1946-1959.
2. Xu, B.P., El Hima, L., Wen, J.X., Dembele, S., Tam, V.H.Y. and Donchev, T., Numerical study on the spontaneous ignition of pressurized hydrogen release through a tube into air, *Journal of Loss Prevention in the process industries*, **21**, No. 2, 2008, pp. 205-213.
3. Wen, J.X., Xu, B.P. and Tam, V.H.Y., Numerical study of spontaneous ignition of pressurized hydrogen release through a length of tube, *Combustion and Flame Journal*, **156**, No. 11, 2009, pp. 2173-2189.
4. Han, S.H., Chang, D. and Kim, J.S., Release characteristics of highly pressurized hydrogen through a small hole, *International Journal of Hydrogen Energy*, **38**, No. 8, 2013, pp. 3503-3512.
5. Velikorodny, A. and Kudriakov S., Numerical study of the near-field of highly underexpanded turbulent gas jet, *International Journal of Hydrogen Energy*, **37**, No. 22, 2012, pp. 17390-17399.
6. Peneau, F., Pedro, G., Oshkai, P., Benard, P. and Djilali, N., Transient supersonic release of hydrogen from high pressure vessel: A computational analysis, *International Journal of Hydrogen Energy*, **34**, No. 14, 2009, pp. 5817-5827.
7. Mohamed, K. and Paraschivoiu, M., Real gas simulation of hydrogen release from a high-pressure chamber, *International Journal of Hydrogen Energy*, **30**, No. 8, 2005, pp. 903-912.
8. Khaksarfard, R. and Paraschivoiu, M., Numerical simulation of high pressure hydrogen release through an expanding opening, *International Journal of Hydrogen Energy*, **37**, No. 10, 2012, pp. 8734-8743.
9. Krothapalli, A., Baganoff, D. and Karamcheti, K., on the mixing of a rectangular jet, *Journal of Fluid Mechanics*, **107**, 1981, pp. 201-220.
10. Makarov, D., Molkov, B., Structure and Concentration Decay in Supercritical Plane Hydrogen jet, Proceedings of the Eighth International Symposium on Hazards, Prevention and mitigation of Industrial explosions, 5-10 September 2010, Yokohama, Japan.
11. Saad, Y., Schultz, M. H., A Generalized Minimal Residual Algorithm for Solving Nonsymmetric Linear Systems, *SIAM Journal of Scientific Computation*, **7**, 1986, pp. 856-869.
12. Khaksarfard, R., Kameshki, M. R. and Paraschivoiu, M., Numerical simulation of high pressure release and dispersion of hydrogen into air with real gas model, *Shock Waves*, **20**, No. 3, 2010, pp. 205-216.
13. Tajallipour, N., Kumar, V., Paraschivoiu, M., Large-eddy simulation of a compressible free jet flow on unstructured elements, *International Journal of Numerical Methods for heat & Fluid*, **23,** No. 2, 2013, pp. 336-354.